



Research Article

Simultaneous estimation of reference temperature and heat transfer coefficient in transient film cooling problems

Vashista ADEMANE^{1,*}, Ravikiran KADOLI¹, Vijaykumar HINDASAGERI²

¹Department of Mechanical Engineering, National Institute of Technology Karnataka, Surathkal, Mangalore, 620015, India

²Consulting Engineer, Quest Global, Belgaum, Karnataka, 560103, India

ARTICLE INFO

Article history

Received: 20 March 2022

Revised: 15 August 2022

Accepted: 29 August 2022

Keywords:

Transient Film Cooling;
Effectiveness; Heat Transfer
Coefficient; Inverse Heat
Conduction Problem;
Levenberg-Marquardt Algorithm

ABSTRACT

This paper aims to simultaneously estimate the reference temperature and heat transfer coefficient in film cooling situations from transient temperature measurements. The existing steady-state technique is a tedious process and employs distinct boundary conditions to evaluate each parameters of the film cooling. Applying different boundary conditions may lead to errors in the estimated parameters due to differences in aerodynamic conditions. On the other hand, a transient technique can estimate both parameters in a single test by utilizing short-duration transient temperature data. Hence, the present study uses a novel approach for solving transient film cooling problems based on the inverse heat conduction approach, which can simultaneously estimate heat transfer coefficient and reference temperature. The present method employs an optimization technique known as the Levenberg-Marquardt Algorithm. The objective function for the inverse algorithm is constructed using the analytical solution of a transient one-dimensional semi-infinite body. The transient surface temperature data required for the present analysis is obtained through a numerical simulation of film cooling arrangement over a flat surface. Laterally averaged effectiveness and heat transfer coefficient for blowing ratios of 0.5, 0.8, and 1.0 are analyzed using the present technique and compared against the steady-state simulation results to demonstrate the methodology. An average deviation of around 7% for the estimated effectiveness and 4% for the heat transfer coefficient values are observed between the present IHCP method and the steady state simulation results. The deviation in heat transfer coefficient predominately occurred near the film hole exit of $x/d < 5$, which might have occurred due to the conjugate solution employed in the present work.

Cite this article as: Ademane V, Kadoli R, Hinasageri V. Simultaneous estimation of reference temperature and heat transfer coefficient in transient film cooling problems. J Ther Eng 2023;9(3):702–717.

*Corresponding author.

*E-mail address: v.ademane@gmail.com

This paper was recommended for publication in revised form by
Regional Editor Ahmet Selim Dalkılıç



INTRODUCTION

Excessive operating temperatures in modern gas turbine engines to improve the Brayton cycle efficiency lead to frequent failure of engine components. Adequate cooling is most desirable in such operating conditions. Film cooling is a typical technique to cool the gas turbine engine components and to protect the surfaces from hot gases. Air as a coolant is issued out of small discreet holes to form a protective layer over the surface. The performance of film cooling is affected by various parameters such as shape, injection angle, blowing ratio, hole length, density ratio [1]. Numerous efforts have been carried out experimentally as well as numerically to study the effect of parameters on film cooling behavior [2]. The flat plate model of film cooling is most commonly used in many studies since it offers less geometric complexity.

The film cooling performance is evaluated by knowing the reduction in the surface heat flux due to film injection. The heat flux (q'') over a film cooled surface mainly depends on the two parameters such as surface heat transfer coefficient (h) and the reference temperature (T_{ref}) of the fluid which can be calculated according to Newton's law cooling as [3],

$$q'' = T_w - T_{ref} \quad (1)$$

The early works on the film cooling used steady-state experimental techniques to evaluate h and T_{ref} [4,5]. In the case of steady-state analysis, these two parameters are evaluated independently by conducting separate experiments for each of the parameters [3]. The reference temperature is calculated by insulating the wall and measuring the adiabatic wall temperature at a steady state. In this case, the free-stream and the coolant will be at different temperatures. While evaluating the heat transfer coefficient, a constant heat flux [6,7] will be applied over the test surface using thin foil heaters and the corresponding wall temperature is measured. Subsequently, using Newton's law of cooling, the heat transfer coefficient is evaluated by keeping the mainstream and the coolant at the same temperature. This method of evaluating heat transfer coefficient has certain limitations, such as maintaining constant heat flux over complex geometries and lateral conduction errors due to longer duration to achieve a steady-state. Also, this method evaluates only one parameter per experiment. Vedula and Metzger proposed a transient technique to estimate h and T_{ref} in case of three temperature convection problems [8]. Later Ekkad et al. used transient liquid crystal thermography to evaluate film cooling effectiveness [9] and heat transfer coefficient [10,11]. They extended their study further using infrared thermography for transient surface temperature measurements [12]. Chen et al. [13] proposed a new data reduction technique based on the transient wall temperature data using liquid crystal thermography to evaluate film cooling parameters.

A new transient technique by applying non-homogeneous heat flux through heater foil was developed by Vogel et al. [14]. They used nonlinear regression to obtain unknown parameters by conducting multiple tests with different heat flux ratios. A major disadvantage of this method is that the applied heat flux influences the thermal boundary layer and affects the heat transfer coefficient. A dual linear regression technique based on a two-test strategy was proposed by Xue et al. for a transonic turbine cascade to determine the recovery temperature, heat transfer coefficient and effectiveness [15]. Ahmed et al. proposed a transient technique for jet impingement studies by solving a three-dimensional heat conduction equation [16]. This technique reduces the lateral conduction error but is computationally more expensive than solving a 1D heat conduction equation. A comprehensive review of recent developments in different techniques used to determine h and T_{ref} for a film cooling problem can be found in Ekkad and Singh [17].

It has been observed that the previous studies followed two or multiple test methods to obtain various parameters. One major drawback of such techniques is the difficulty in maintaining the same aerodynamic conditions when different boundary conditions are applied. Hence it is essential to develop a method that can determine both h and T_{ref} from a single transient test. Solutions to such problems can be obtained using the inverse heat transfer approach.

The inverse heat conduction problems (IHCP) in heat transfer are related to estimating the unknown parameters such as boundary conditions, initial conditions, or the thermophysical properties using transient temperature measurements [18]. When the boundary conditions at a surface are known, it is possible to find the temperature distribution on a surface. This technique is known as the direct problem. On the other hand, in the case of inverse problems, the boundary conditions are estimated by measuring the temperature-time history [19]. The difficulty in the case of IHCPs is that the solution is ill-posed. Hence the solution to IHCPs is very sensitive to the errors in the measurements. Different methods have been proposed for the solution of IHCPs, such as Tikhonov's regularization technique, Beck's function estimation, optimization technique, Genetic algorithm, etc. [20]. Inverse solutions are majorly classified as stochastic and gradient-based methods [21]. Stochastic methods can find the global minimum but are complicated to implement and require many iterations to converge. Contrarily, the gradient-based methods are faster in convergence and simple to implement, but they may result in local minima. The difficulty associated with the gradient-based method is calculating the sensitivity coefficients accurately when the inverse problem is nonlinear. Levenberg-Marquardt Algorithm (LMA) is one of the most straightforward yet robust method used for solving inverse heat conduction problems based on optimization technique. It is a gradient-based method that combines the steepest descent

method in the neighborhood of the initial guess and uses the Gauss-Newton method near the minimum of the ordinary least squares norm [22]. LMA was successfully applied by numerous researchers to estimate thermophysical properties and boundary conditions [23,24]. Even the most modern technologies, such as neural networks, use LMA as a training algorithm [25].

Computational fluid dynamics (CFD) is one of the most effective methods for investigating complex flow phenomena in various applications [26]. A study on the flow pattern and heat transfer characteristics through CFD was investigated for a circular tube with a twisted tape insert by Al-Obaidi and Cahaer [27]. Later this study was extended using dimpled and corrugated tube surfaces [28,29]. Additionally, a numerical study on the influence of various configurations of corrugated pipes was done to conduct a heat transfer analysis, which showed that higher corrugation ratios could result in higher heat transfer rates [30–32]. Based on the numerical outcome, correlations have been developed for friction factor, Nusselt number and performance factor [33]. Further, Alhamid and Al-Obaidi used Al_2O_3 based nanofluid in a dimpled circular tube to investigate the hydrodynamic thermal characteristics using ANSYS Fluent [34]. Similarly, CFD techniques are successfully applied to evaluate h and T_{ref} in case of film cooling situations [35,36] and also used to develop novel hole shapes to increase the cooling performance. Most of the numerical studies related to film cooling have considered an adiabatic surface to calculate the effectiveness. However, the velocity field might get influenced by the heat transfer between the fluid and the surface [37]. A conjugate calculation can include this effect and may lead to accurate prediction of film cooling parameters [38]. It is observed that the conjugate solution results in an underprediction of the absolute temperatures than the experimental results [39]. Hence a conjugate numerical simulation of the film cooling situation could be more realistic than the existing adiabatic film cooling assumptions.

It is observed from the literature that a transient film cooling analysis can quickly predict both the heat transfer coefficient and reference temperature. Also, a significant advantage of conducting a transient study is that it can replace the two-test strategy of steady-state analysis. The existing transient studies have also followed the two-test method due to difficulties associated with the data reduction technique. Hence, developing a data reduction technique for the transient analysis of film cooling situations using a single test approach is essential. Based on the above observations, the present work aims to achieve a few objectives, such as conducting a transient analysis to evaluate boundary parameters for a film cooling problem. To develop an approach to obtain film cooling effectiveness and heat transfer coefficient using short duration transient data from a single test that is accurate and easy to

implement. Also, it is essential to study the effect of transient data on the solution approach.

Hence in the present work, the feasibility of simultaneously estimating the convective heat transfer coefficient and reference temperature in case of film cooling problems through a single transient experiment is attempted. The novelty of the present work lies in the proposed data reduction method, which is based on the inverse heat conduction approach. This method can solve and evaluate multiple film cooling parameters using a single set of transient data. The proposed method utilizes the analytical solution of the transient one-dimensional semi-infinite heat conduction model as the forward solution. The inverse solution is obtained using an optimization technique known as Levenberg-Marquardt algorithm. A conjugate numerical simulation is performed in ANSYS Fluent to generate transient wall temperature data required for the analysis. The film cooling parameters, h and T_{ref} are evaluated through an in-house MatLab code using transient data obtained from the simulations. Results from the present technique are validated with the results obtained from steady-state numerical simulation for blowing ratios of 0.5, 0.8, and 1.0. A brief discussion on the sensitivity of input data on the current solution approach in estimating film cooling parameters is also presented.

ONE DIMENSIONAL SEMI-INFINITE ANALYSIS

Figure 1 shows a typical film cooling arrangement over a flat surface. The aim here is to calculate the local fluid temperature (T_{ref}) and heat transfer coefficient (h) over the surface using the transient temperature measured at $y = 0$. This problem can be simplified by assuming the plate as a semi-infinite model with one-dimensional heat conduction across the thickness of the plate. But the semi-infinite assumption is valid only for a short duration such that the temperature change on the top surface ($y = 0$) should not affect the bottom surface temperature (i.e., at $y = L$, $T_w = T_i$) [14].

The general governing equation for one dimensional transient heat conduction through a semi-infinite flat plate with a convection boundary condition on one side can be written as [40],

$$k \frac{\partial^2 T}{\partial y^2} = \frac{1}{\alpha} \frac{\partial T}{\partial t} \quad (2)$$

The boundary conditions are as follows,

$$\text{at } y = 0, -k \frac{\partial T}{\partial y} = h(T_w - T_{ref}) \quad (3)$$

$$\text{as } y \rightarrow \infty, T = T_i \quad (4)$$

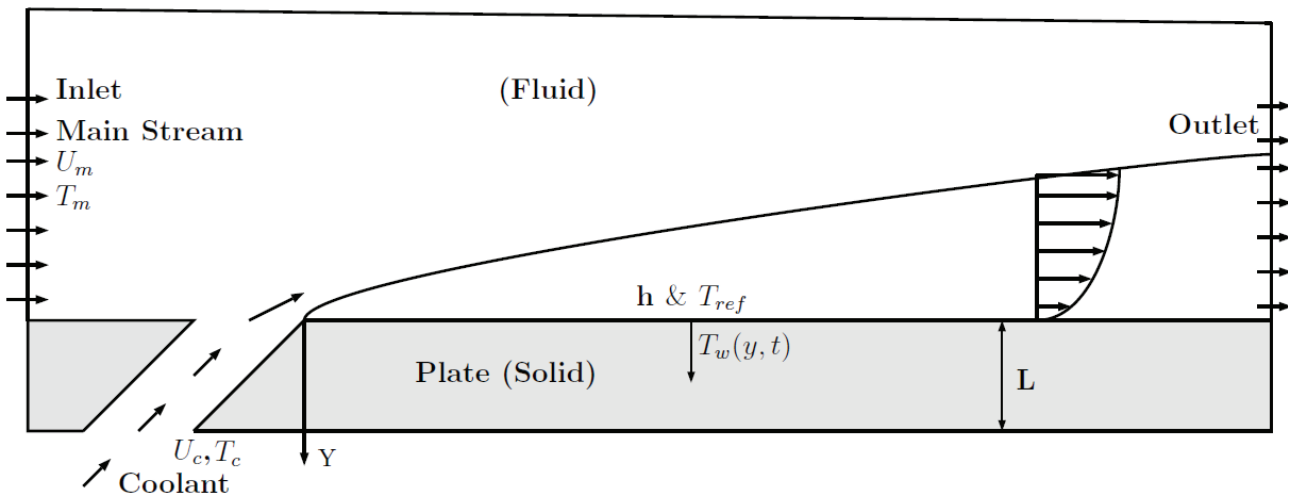


Figure 1. Film cooling arrangement over a surface of flat plate and the one-dimensional heat transfer across the thickness of the plate.

The reference temperature in Equation 3, T_{ref} is the mixture temperature of the mainstream and coolant over the film cooled surface, and T_w is the temperature of the plate.

The initial condition is given by,

$$at\ t = 0, T = T_i \quad (5)$$

The solution for Equation 2 using the prescribed initial and boundary conditions is given by [40],

$$\frac{T_w(y, t) - T_i}{T_{ref} - T_i} = \operatorname{erfc}\left(\frac{y}{2\sqrt{\alpha t}}\right) - \exp\left(\frac{hy}{k} + \frac{h^2 \alpha t}{k^2}\right) \operatorname{erfc}\left(\frac{y}{2\sqrt{\alpha t}} + \frac{h\sqrt{\alpha t}}{k}\right) \quad (6)$$

where α and k are the thermal diffusivity and thermal conductivity of the plate material respectively.

In case of jet in cross-flow situations such as film cooling, a coolant stream is injected into the mainstream as represented in Figure 1. Hence the fluid temperature in the downstream of injection is a mixture of two fluid streams. This mixture temperature is unknown and has to be evaluated, which is attributed as reference temperature (T_{ref}). The reference temperature is highly localized with respect to the location and depends on the mixing phenomena of hot and cold fluids. In case of film cooling arrangement, T_{ref} is represented in terms of a non-dimensional quantity known as effectiveness (η), which is defined as [4],

$$\eta = \frac{T_{ref} - T_m}{T_c - T_m} \quad (7)$$

where T_c and T_m are the temperatures of the coolant and mainstream, respectively. Equation 6 has two unknowns (h and T_{ref}) which necessitates one more additional equation to evaluate the two parameters. Since only one equation is available, the solution for this problem can be obtained

through an iterative technique with nonlinear least squares regression.

LEVENBERG-MARQUARDT ALGORITHM

To evaluate film cooling unknown boundary parameters, h and T_{ref} existing in Equation 6, one of the robust optimization technique known as the Levenberg-Marquardt algorithm (LMA) is used in the present study. LMA is an iterative approach that evaluates the optimum values of unknown parameters by minimizing the variance between the measured and the estimated temperatures.

Firstly the inverse problem needs to be constructed by defining an objective function (S) defined as the summation of the squared difference between the measured and the estimated temperatures [18], which can be written as Equation 8,

$$S(P) = \sum_{i=1}^I [Y_i - T_i(P)]^2 \quad (8)$$

where Y and T are the measured and estimated temperatures at a particular location (x/d) and the subscript $i = 1, 2, 3, 4, \dots, I$. The estimated temperature values are obtained by solving Equation 6. The term P refers to the unknown parameters, T_{ref} and h in the present case. The objective function S is in the form of ordinary least squares norm. In order to minimize the objective function, the derivatives of Equation 8 with respect to the unknown parameters need to be evaluated and equated to zero [18].

$$\frac{\partial S(P)}{\partial P} = 0 \quad (9)$$

Equation 9 can be represented in the form of matrix notation as follows,

$$-2J(P)[Y - T(P)] = 0 \quad (10)$$

where, $J(P) = \frac{\partial T^T(P)}{\partial P}$ is known as Jacobian or the sensitivity coefficient, which is defined as the rate of change of the dependent variable with respect to the unknown parameters. In the present work, the sensitivity coefficients are evaluated by the direct differentiation of Equation 6 with respect to h and T_{ref} . The expressions obtained to calculate the sensitivity coefficients are as follows,

$$J(T_{ref}) = \frac{\partial T_w}{\partial T_{ref}} = \operatorname{erfc}\left(\frac{y}{\sqrt{4\alpha t}}\right) - \exp\left(\frac{hy}{k} + \frac{h^2\alpha t}{k^2}\right) \operatorname{erfc}\left(\frac{y}{\sqrt{4\alpha t}} + \sqrt{\frac{h^2\alpha t}{k^2}}\right) \quad (11)$$

$$J(h) = \frac{\partial T_w}{\partial h} = (T_i - T_{ref}) \left[\left(\frac{y}{k} + \frac{2h\alpha t}{k^2} \right) \exp\left(\frac{hy}{k} + \frac{h^2\alpha t}{k^2}\right) \operatorname{erfc}\left(\frac{y}{\sqrt{4\alpha t}} + \sqrt{\frac{h^2\alpha t}{k^2}}\right) - \sqrt{\frac{4\alpha t}{\pi k^2}} \exp\left\{ \frac{hy}{k} + \frac{h^2\alpha t}{k^2} - \left(\frac{y}{\sqrt{4\alpha t}} + \sqrt{\frac{h^2\alpha t}{k^2}} \right)^2 \right\} \right] \quad (12)$$

The inverse problem becomes nonlinear if the Jacobian has a functional dependency on the unknown parameters. The solution to Equation 10 is obtained through an iterative procedure. Here the vector $T(P)$ is linearized using the Taylor series of expansion with respect to iteration κ as [18],

$$T(P) = T(P^\kappa) + J(P^\kappa)(P - P^\kappa) \quad (13)$$

Substituting the Equation 13 in Equation 10 and after some rearrangement yields the following expression for the unknown parameters, P [18]:

$$P^{\kappa+1} = P^\kappa + [(J^\kappa)^T J^\kappa]^{-1} (J^\kappa)^T [Y - T(P^\kappa)] \quad (14)$$

Equation 14 is known as Gauss-Newton method, which is an approximation of the Newton's method. When $|J^T J|$ in Equation 14 becomes very small or zero, the inverse problem becomes ill-conditioned, and the parameter estimation is impossible. This difficulty has been overcome by introducing a positive scalar known as damping parameter (λ) to Equation 14 as [18],

$$P^{\kappa+1} = P^\kappa + [(J^\kappa)^T J^\kappa + \lambda^\kappa \Omega^\kappa]^{-1} (J^\kappa)^T [Y - T(P^\kappa)] \quad (15)$$

The Equation 15 is known as Levenberg-Marquardt method. The term Ω is a diagonal matrix which is calculated as follows [18],

$$\Omega^\kappa = \operatorname{diag}[(J^\kappa)^T J^\kappa] \quad (16)$$

The value of the damping parameter, λ , used in Equation 15 is made large during the initial iterations so

that the oscillations due to ill-conditioning will be damped, and the solution tends to the steepest descent method. As the iteration progresses, the value of λ will be reduced, and the solution follows the Gauss-Newton method. Stopping criteria for the iterations is given by [18],

$$|P^{\kappa+1} - P^\kappa| < 10^{-3} \quad (17)$$

$$|S(P^{\kappa+1})| < 10^{-3} \quad (18)$$

The flow chart of the in-house MatLab code to find the unknown film cooling parameters using the present IHCP technique is given in Figure 2.

NUMERICAL EVALUATION OF TRANSIENT TEMPERATURE DATA

The transient surface temperature data required for the present IHCP technique is obtained from a three-dimensional numerical simulation using ANSYS Fluent. The geometrical parameters of the computational domain are specified following the experimental work of Sinha et al. [41]. Figure 3 shows a half section of the computational domain with the dimensions normalized using the film cooling hole diameter, d . The computational domain is divided into a solid region made up of film cooled plate with an inclined hole and a fluid region which contains a mainstream, a plenum chamber, and the fluid inside the film hole. Mainstream at higher temperatures enters and exits the domain through the inlet and outlet boundary surfaces as shown in Figure 3. At the inlet of the mainstream, velocity and temperature values are specified, and zero relative pressure boundary condition is set at the outlet. The coolant enters through the bottom surface of the plenum chamber and exits through the film hole into the mainstream. The coolant inlet boundary condition is specified with a mass flux having a particular temperature.

Table 1. Input conditions used in the present simulation

Parameter	Values
Diameter of the jet, d	12.7 mm
Angle of injection, α	35°
Pitch, P/d	3
Length of hole, L/d	1.74
Mainstream velocity, U_m	20 m/s
Mainstream temperature, T_m	600K
Jet Temperature, T_c	300K
Blowing Ratio ($M = \frac{\rho_c U_c}{\rho_m U_m}$)	0.5 and 1.0
Thickness of the plate, L	10 mm

The coolant mass flux is calculated based on the required blowing ratio at the hole exit [42–44], which is defined as the ratio of mass fluxes of the coolant to the mainstream. Symmetry boundary condition is applied on the lateral sides of the mainstream and the plenum chamber. The bottom and the lateral surfaces of the plate are insulated. The origin ($x = y = z = 0$) is located at the trailing edge of the film hole exit. Table 1 shows the details of the input conditions used in the present simulation.

The computational domain is discretized using unstructured tetrahedron elements. Inflation layers are generated above the film cooling surface with a y^+ value approximately equal to 15. Figure 4 depicts the results of a grid independence analysis for four different mesh refinements of 1.8, 2.5, 3.9, and 6.8 million elements. It can be observed from the figure that the deviation in the computed effectiveness is minimal for all mesh configurations. About 2% variation in the effectiveness is observed for $2 < x/d < 4$, and in the rest of the locations, the deviation lies below 1%. An

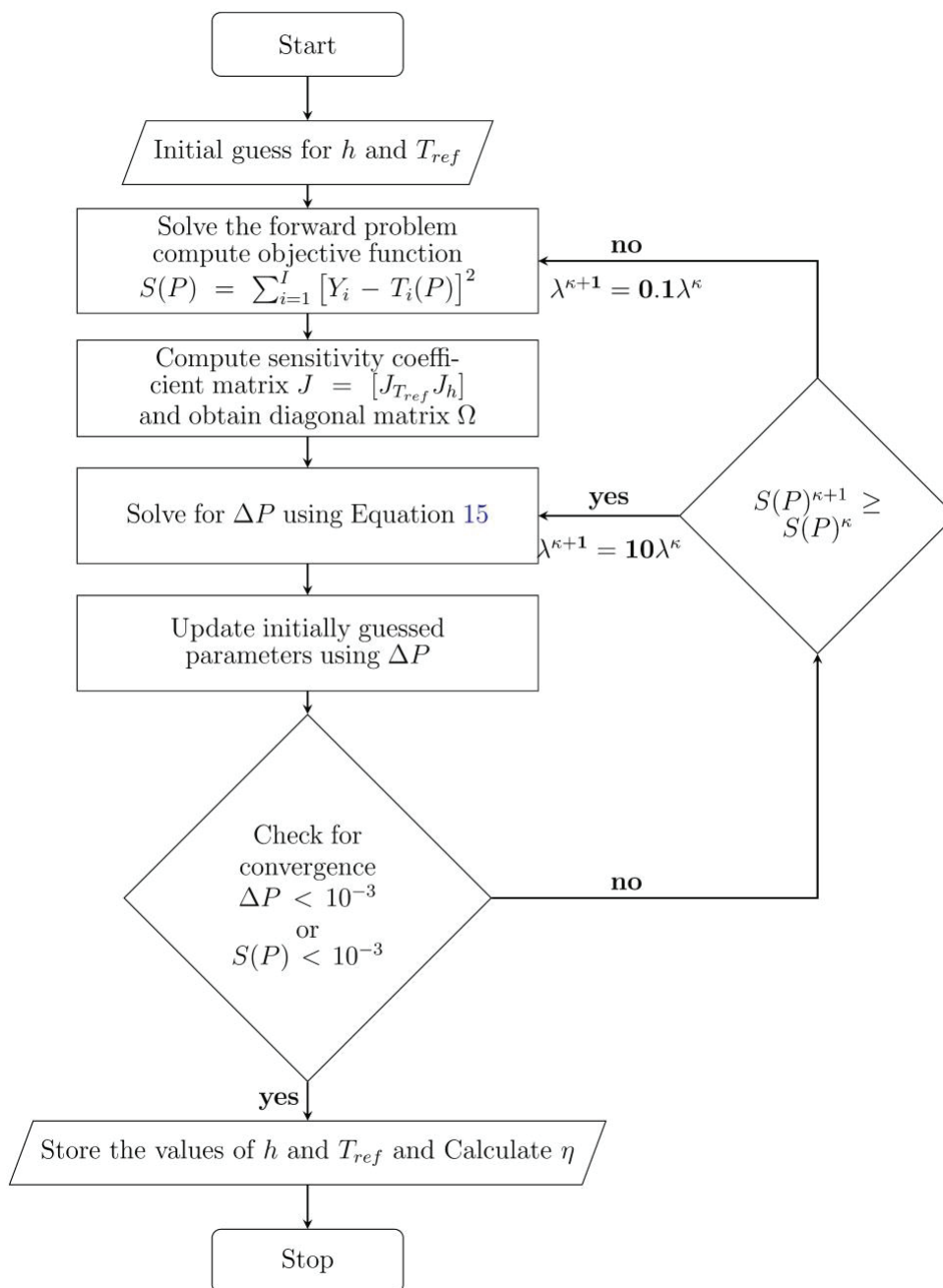


Figure 2. Flow chart of the present inverse algorithm for the estimation of film cooling parameters.

average deviation in the computed effectiveness between 1.8 and 6.8 million elements is around 0.7%. Hence all further simulations are conducted for mesh configuration having 2.5 million elements. This specific mesh configuration ensures better spatial distribution while maintaining a reasonable computation time.

Three-dimensional Reynolds Averaged Navier-Stokes (RANS) equations are solved along with standard $k - \epsilon$ turbulence model with standard wall functions. The convective components are discretized using a second-order upwind interpolation approach, and pressure-velocity coupling is accomplished using the SIMPLE algorithm. Also, temporal discretization is achieved through a second-order implicit scheme. The transient simulation is carried out for about 200 seconds with a time step of 0.01 seconds.

The numerical simulation considers a film cooling plate with a thickness (L) of 10mm. The thermo-physical properties of the plate materials are similar to the properties of Polymethylmethacrylate (PMMA) or acrylic material. The thermal conductivity (k) and thermal diffusivity (α) of the plate material are 0.187 W/m-K and 1.076×10^{-7} m²/s respectively. Due to its low thermal conductivity, the acrylic plate allows transient temperature measurements for a longer duration without violating the semi-infinite assumption. Most of the studies on transient film cooling have used an acrylic plate for transient surface temperature measurements [12]. In the present work, the transient wall temperature data at $y/d = 0$ is stored every 0.1 seconds for $x/d = 0 - 30$. The simulation is started with an initial

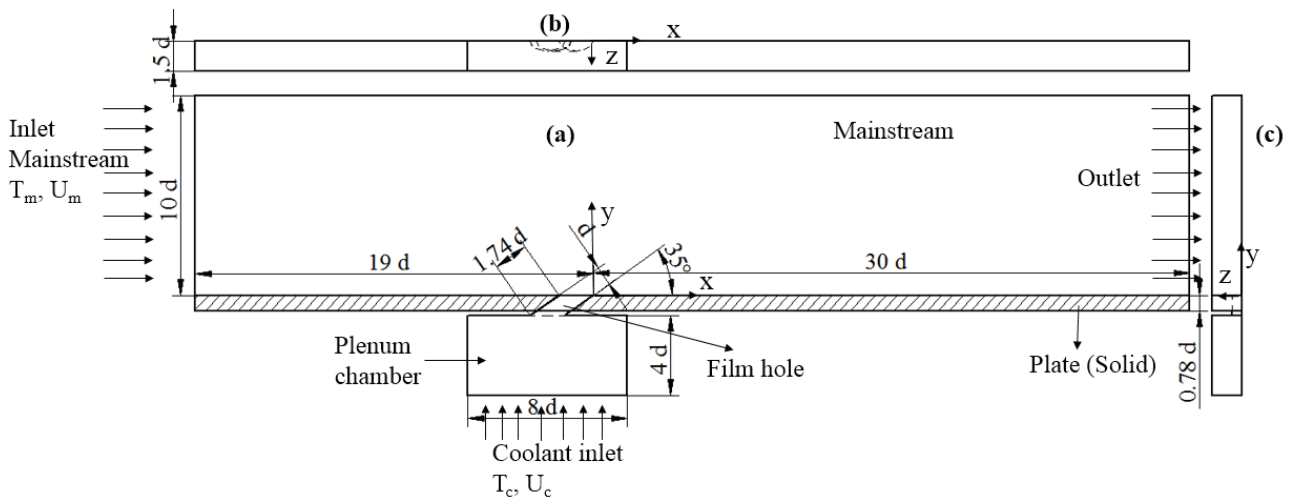


Figure 3. A 2D representation of the computational domain used for transient analysis film cooling over a flat surface. (a) Front sectional view at $z/d = 0$ (b) Top view, and (c) Side view.

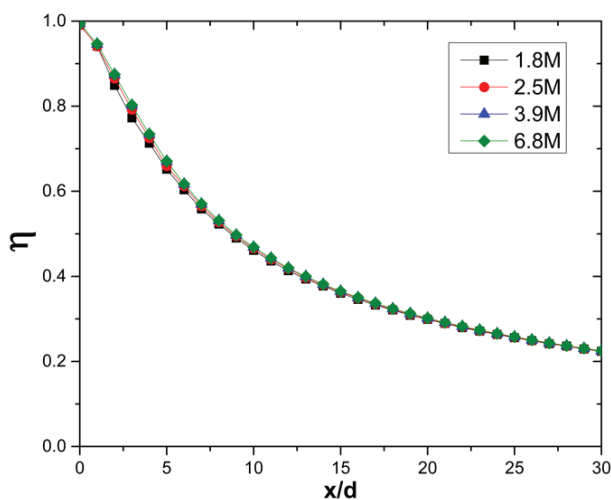


Figure 4. Effect of mesh refinements on computed effectiveness by numerical simulation for $M = 0.5$.

temperature of 300K for the solid domain such that at $t = 0$, $T = T_i$ is maintained.

The plate can be assumed semi-infinite only if it satisfies the condition $T = T_i$ at $y = L$. The diffusive time constant ($\tau_{diff} \approx \frac{L^2}{4\alpha t}$) evaluates the time taken by the thermal wave to travel from the top surface ($y = 0$) to bottom surface ($y = L$) [45]. For the PMMA material used in the present simulations, the τ_{diff} is obtained around 232 seconds. In the present IHCP technique, transient data from 20-100 seconds are used to estimate the film cooling parameters. Hence the semi-infinite assumption used in the present study is justifiable concerning the sampling duration of transient temperature data.

The two fluid streams, mainstream and coolant, have different temperatures in the present case. Hence the variation of thermophysical parameters of the fluid corresponding to temperature are included while setting up the

Table 2. Coefficients of the curve fit equation for the variation of fluid properties with respect to temperature

$f(T)$	α_0	α_1	α_2	α_3
$k(T)$	3.6404×10^{-4}	9.8947×10^{-5}	-4.5763×10^{-8}	1.3974×10^{-11}
$\mu(T)$	1.8115×10^{-6}	6.4977×10^{-8}	-3.5017×10^{-11}	9.7110×10^{-15}
$C_p(T)$	961.29	9.5836×10^{-2}	1.3649×10^{-4}	-5.7898×10^{-8}

problem in Fluent. The density variation of air is included based on the assumption of incompressible ideal gas. Other properties such as thermal conductivity, dynamic viscosity, and specific heat are given as a function of temperature [46]. A third order polynomial curve is fitted for these three parameters with temperature and the coefficients of the curve fit equation are given as input to the fluent while defining the material properties of the fluid. The third order polynomial equation used for the curve fit in the present study is written as,

$$f(T) = a_0 + a_1T + a_2T^2 + a_3T^3 \quad (19)$$

The coefficients of polynomial equation are given in Table 2.

RESULTS AND DISCUSSION

Validation of the Numerical Setup and the Present IHCP Method

At first, the numerical solution results are validated against the experimental results of Sinha et al. (1991). A steady-state simulation is carried out for blowing ratios of 0.5 and 1.0. Figure 5 compares the centerline effectiveness obtained from the steady-state simulation with the

experimental results of [41] for $M = 0.5$ and 1.0. There is a close agreement with the experimental results that exists up to $x/d = 15$ with an average error of around 5%. However, the deviation gradually increases further downstream ($x/d > 15$), resulting in an average error of 19%. At $M = 1.0$ the deviation is observed to be around 8% up to $x/d = 30$.

The experimental result for $M = 1.0$ shows a sudden drop in the effectiveness values at $x/d = 2.5$ and increases slightly till $x/d = 7$ and then decreases further downstream. This is due to jet separation and reattachment, which occurs at blowing ratio of 1. In film cooling, the jet-mainstream interaction creates a distinctive flow feature known as counter rotating vortex pair (CRVP). The lift-off of the coolant jet is mostly caused by the presence of CRVP, whose strength rises as the blowing ratio increases. Hence, exact prediction of film cooling behaviour in numerical simulation becomes extremely difficult. It appears in the present simulation, the jet separation and the reattachment phenomena are not captured precisely. However, an overall film cooling behaviour is roughly apprehended.

Previous numerical works have also observed the downstream deviation of numerical results from the experimental results. One primary reason is attributed to the isotropic turbulence viscosity assumption causing an overprediction in the computed centerline effectiveness [36]. Also, it was reported that the sources of errors could be the possibility

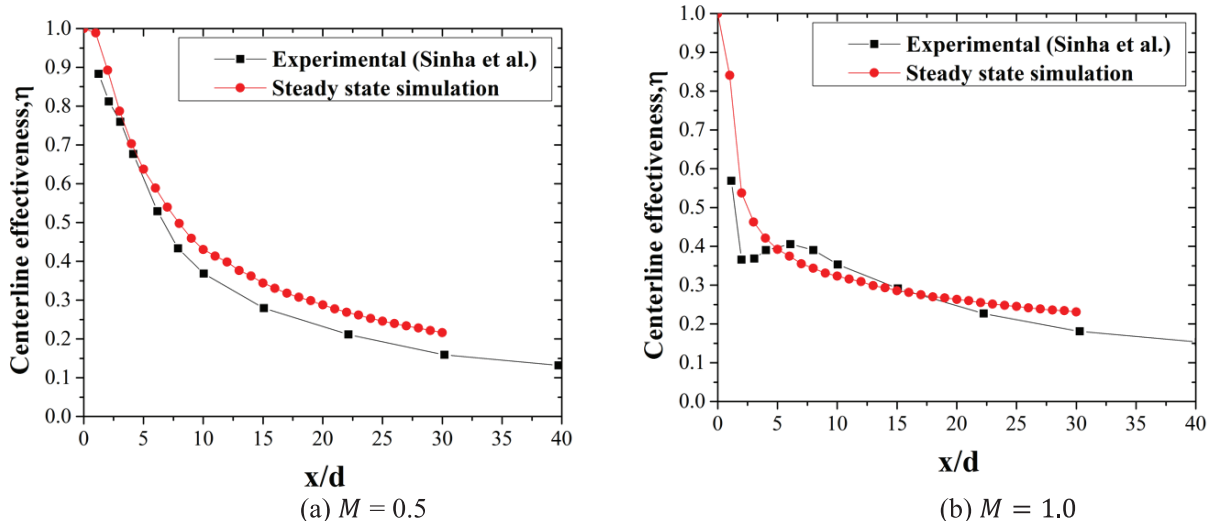


Figure 5. Validation of the present numerical results with the literature.

of jet skewness [35], lateral conduction errors during the experiments [47], use of tetrahedral meshes and inappropriate wall functions [48].

A validation of the present IHCP method is performed using the experimentally obtained h and T_{ref} values from Chen et al. (2001) [13] for $M = 0.5$. The values of h and T_{ref} from [13] are used to generate transient temperature from one-dimensional semi-infinite solution given in Equation 6. A random noise of ± 1 K is introduced to the transient wall temperature generated using Equation 6 to obtain noisy data. Then from the present IHCP technique, the effectiveness and heat transfer coefficients were estimated using the noisy data. Figure 6(a) shows the transient temperature generated from the solution of direct problem at $x/d = 10$ along with externally added random noise of ± 1 K. Figure 6(b) and Figure 6(c) shows the comparison of estimated parameter values with corresponding experimental values. It was found that the present IHCP technique has estimated the parameters accurately with an average error of less than 1% from the noisy data. It is observed that higher noise levels increase the deviation in the estimated

parameters. When a noise of ± 5 K is introduced to the input data, the estimated parameters have deviated with more than 10% error.

Linear Fit Method

When the transient surface heat flux data is available, it is possible to estimate the unknown film cooling parameters using the linear relation between the wall temperature and the surface heat flux data. The linear relation can be obtained using Newton's law of cooling as [49],

$$q''(t) = h(T_w(t) - T_{ref}) \quad (20)$$

This equation can be rewritten as [49],

$$T_w(t) = \frac{q''(t)}{h} + T_{ref} \quad (21)$$

The Equation 21 is in the form of $y = mx + c$, where the slope, $m = 1/h$ and the y-intercept is T_{ref} . By plotting transient heat flux vs wall temperature both heat transfer

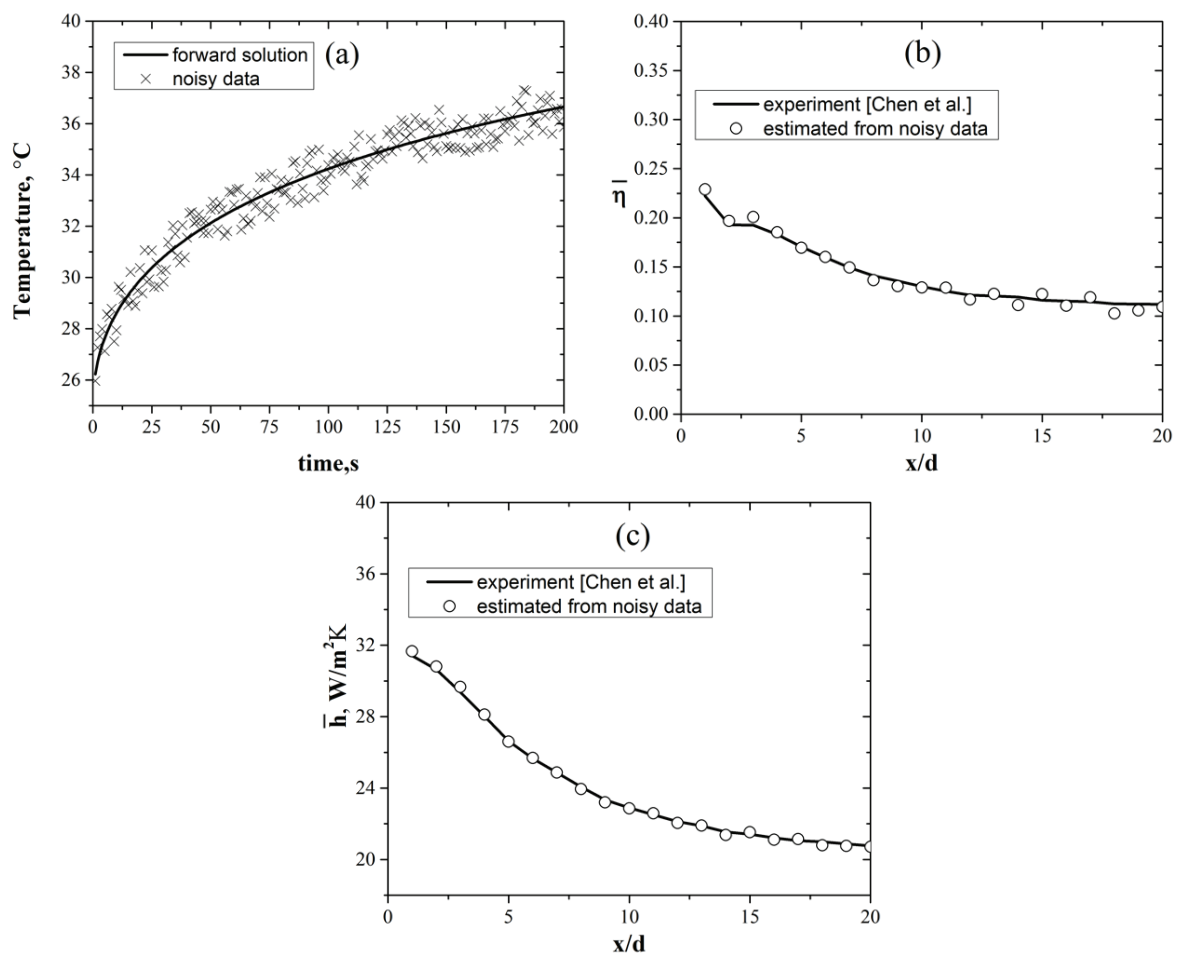


Figure 6. (a) Transient temperature data generated from the forward solution with additional random noise of ± 1 K, comparison of estimated parameters using noisy data (b) effectiveness, (c) heat transfer coefficient.

coefficient and the reference temperature can be obtained by finding the slope and the y -intercept respectively. Figure 7 shows the linear relation between wall temperature and heat flux at different x/d by plotting $q''(t)$ vs $T_{wall}(t)$.

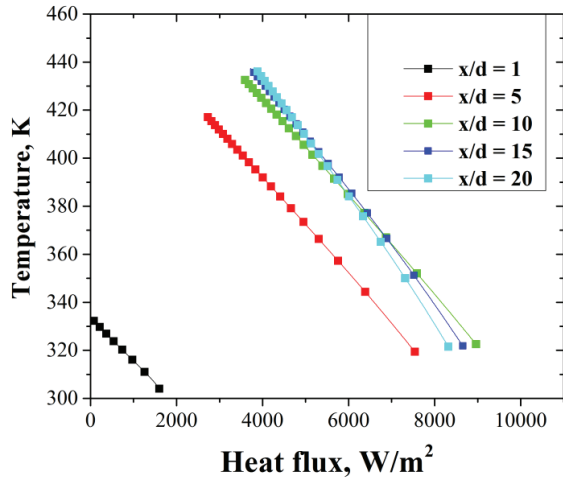


Figure 7. Linearity between wall temperature and heat flux.

Effectiveness

Laterally averaged effectiveness estimated from the present IHCP technique for blowing ratios of 0.5, 0.8 and 1.0 are shown in Figure 8. The jet direction is mostly determined by the blowing ratio, which influences the distribution of the coolant and there by affecting the effectiveness. At low blowing ratio ($M = 0.5$), the $\bar{\eta}$ reduces gradually along the length. As M increases, the coolant jet issues out with more momentum, causing low values of $\bar{\eta}$. It can be noted from the figure that the rate of reduction of $\bar{\eta}$ is less for $M = 1$ than $M = 0.5$. At $M = 1$, $\bar{\eta}$ drastically reduces for $x/d < 15$ and thereafter appears to have a negligible variation along x/d .

The estimated $\bar{\eta}$ values are compared with the steady-state simulation results for corresponding blowing ratios. In steady-state analysis, the film cooling surface is insulated while evaluating its effectiveness. The adiabatic wall temperature yields the local fluid temperature at steady-state. Figure 8 also presents the $\bar{\eta}$ obtained using the method of linear fit as discussed in the previous section. It is observed that $\bar{\eta}$ values estimated using the present IHCP technique are in good agreement with steady-state simulation results

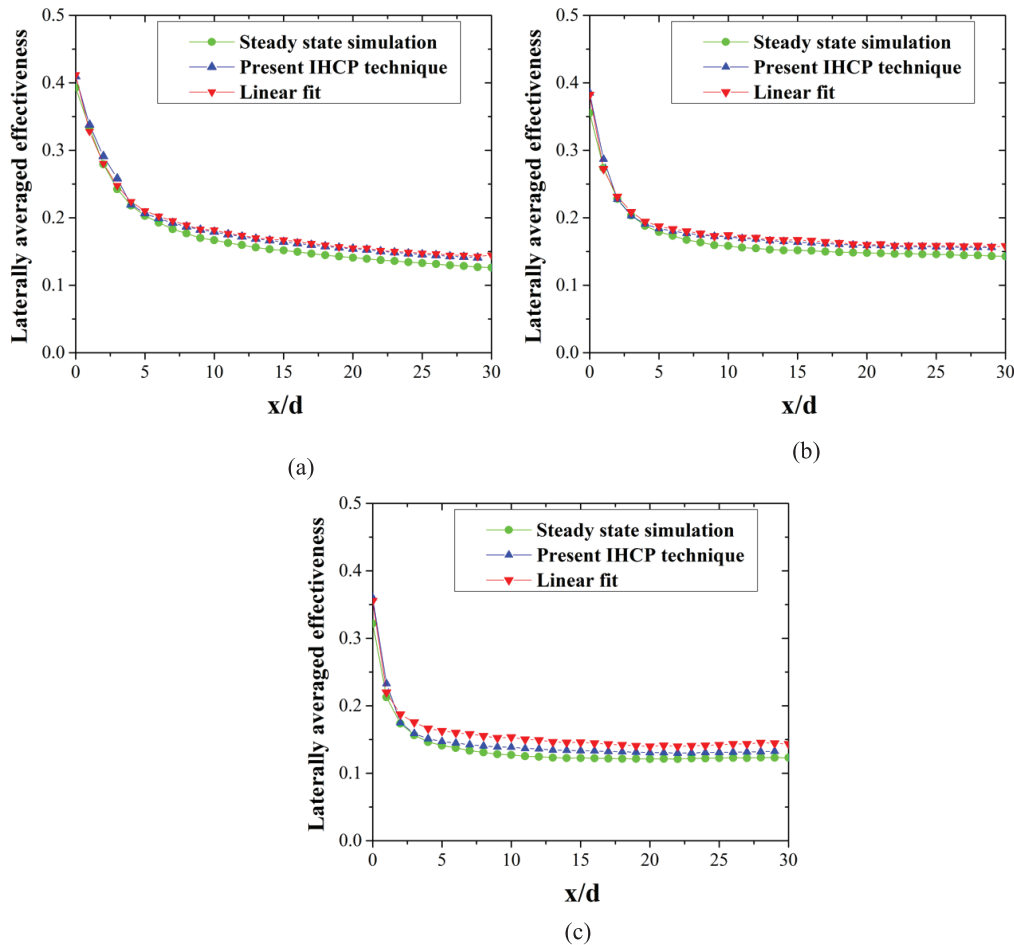


Figure 8. Comparison of laterally averaged effectiveness obtained using different techniques for (a) $M = 0.5$, (b) $M = 0.8$ and (c) $M = 1.0$.

linear fit method. Average deviation between the steady-state and the present IHCP solution is around 6% - 7% for all blowing ratios. The estimated values are in close agreement till $x/d \approx 7$ with an error less than 5% and slightly increases thereafter. Results obtained from the IHCP solution are almost coincides with the output of liner fit method. The deviation between the linear fit method and steady-state analysis is around 8% for $M = 0.5$ and 0.8, but slightly increases to 12% for $M = 1$. One major disadvantage of the linear fit method is that it requires transient heat flux values along with wall temperature to compute the parameters. The accurate measurement of surface heat flux is very challenging, hence the linear fit method might produce results with higher uncertainty.

Sensitivity Analysis

To avoid the ill-conditioned problem, the values of sensitivity coefficients must have large magnitudes [18]. Figure 9 shows the sensitivity coefficient values for reference temperature and heat transfer coefficient with time. The sensitivity coefficients can be calculated either by direct differentiation or numerical differentiation. If the forward solution is simple, then direct differentiation is possible. In the present work analytical solution to the one-dimensional heat conduction equation is used as a forward model. Instead, the sensitivity coefficients may have to be evaluated using numerical differentiation if a three-dimensional governing equation is considered. However, the numerical differentiation is computationally expensive and less accurate than direct differentiation. In such situations, the use of other optimization techniques which are independent of Jacobian evaluation can be implemented.

In the present case, the values of $J_{T_{ref}}$ and J_h are calculated using Equation 11 and 12, respectively. Both $J_{T_{ref}}$ and J_h values are increasing with time, but $J_{T_{ref}}$ values are lower than J_h values. This indicates that the estimated temperature is less sensitive to change in reference temperature than the heat transfer coefficient, which makes the estimation of effectiveness more difficult than h . An immediate conclusion is that the least square error between the exact and estimated values for heat transfer coefficient would be less than the effectiveness. Also, from Figure 9, it is noted that the magnitudes of sensitivity coefficients are very small during the initial time. Hence considering transient data for a concise duration may lead to inaccurate parameter estimation. It can be observed from the Equation 11 and 12 that $J_{T_{ref}}$ is dependent only on estimated h , but J_h is a function of both T_{ref} and h values indicating both the parameters are linearly dependent.

The determinant of $J^T J$ is plotted with time in Figure 10 to compare the effect of sampling rate. Transient data is sampled with a time interval of 0.1, 1, 5 and 10 seconds. The figure indicates a steep rise in the magnitude of $|J^T J|$ up to around 20 seconds and gradually increases further. Hence the transient data considered below this point would increase the uncertainty in the parameter estimation. One

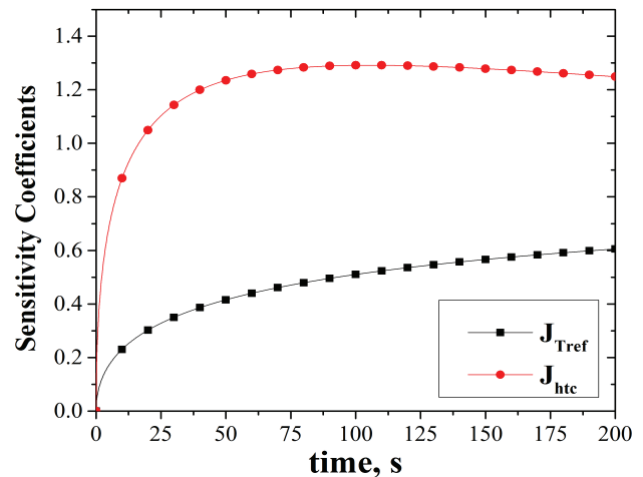


Figure 9. Sensitivity coefficients for T_{ref} and h with time at $x/d = 10$ for $M = 1.0$.

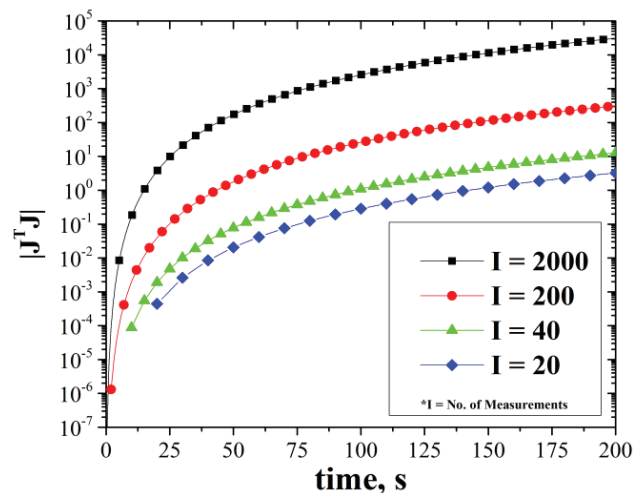


Figure 10. Determinant of sensitivity coefficients with time at $x/d = 10$ for $M = 1.0$.

of the significant observations from the figure is that higher values of $|J^T J|$ can be obtained by increasing the rate of sampling. Hence it can be concluded that, even with a short duration of the transient experiment, the parameter estimation uncertainty can be reduced using a higher sampling rate.

Heat Transfer Coefficient

In the case of film cooling, the heat transfer coefficient is normalized by the heat transfer coefficient over a flat plate with no coolant injection (h_0). Therefore, it is essential to calculate the heat transfer coefficient for a non-film cooling flat plate case. A steady-state numerical simulation is performed for this particular case by specifying a surface heat flux (q'') of 1000 W/m² throughout the plate. The plate dimensions are kept as that of the solid domain

as mentioned in the Figure 3. In addition, h_0 is calculated using the Nusselt number correlation for turbulent boundary layer over a flat plate with constant heat flux boundary condition as [46],

$$Nu = \frac{h_0 x}{k} = 0.0308 Re_x^{(4/5)} Pr^{(1/3)} \quad (22)$$

The fluid properties such as ρ , μ , and Pr in case of correlation are evaluated at an average temperature using the property table available in Incropera et al. (2006) [46]. The average fluid temperature is calculated using free-stream temperature and average temperature of the wall subjected to constant heat flux boundary condition obtained from steady-state simulation.

Now, heat transfer coefficient values for non-film cooling flat plate case are estimated from the present IHCP technique and validated with the steady-state numerical simulation results and the values obtained from the correlation given in Equation 22. Therefore a conjugate transient

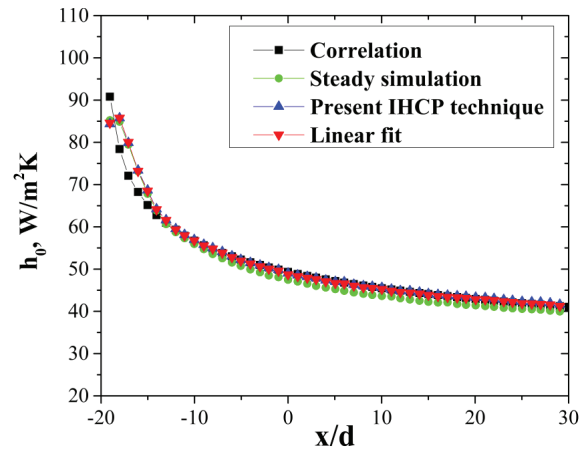


Figure 11. Heat transfer coefficient for a flat surface with no coolant injection.

numerical simulation is conducted and using the transient wall temperature data, h_0 values are estimated by employing the present IHCP approach. The linear fit method is

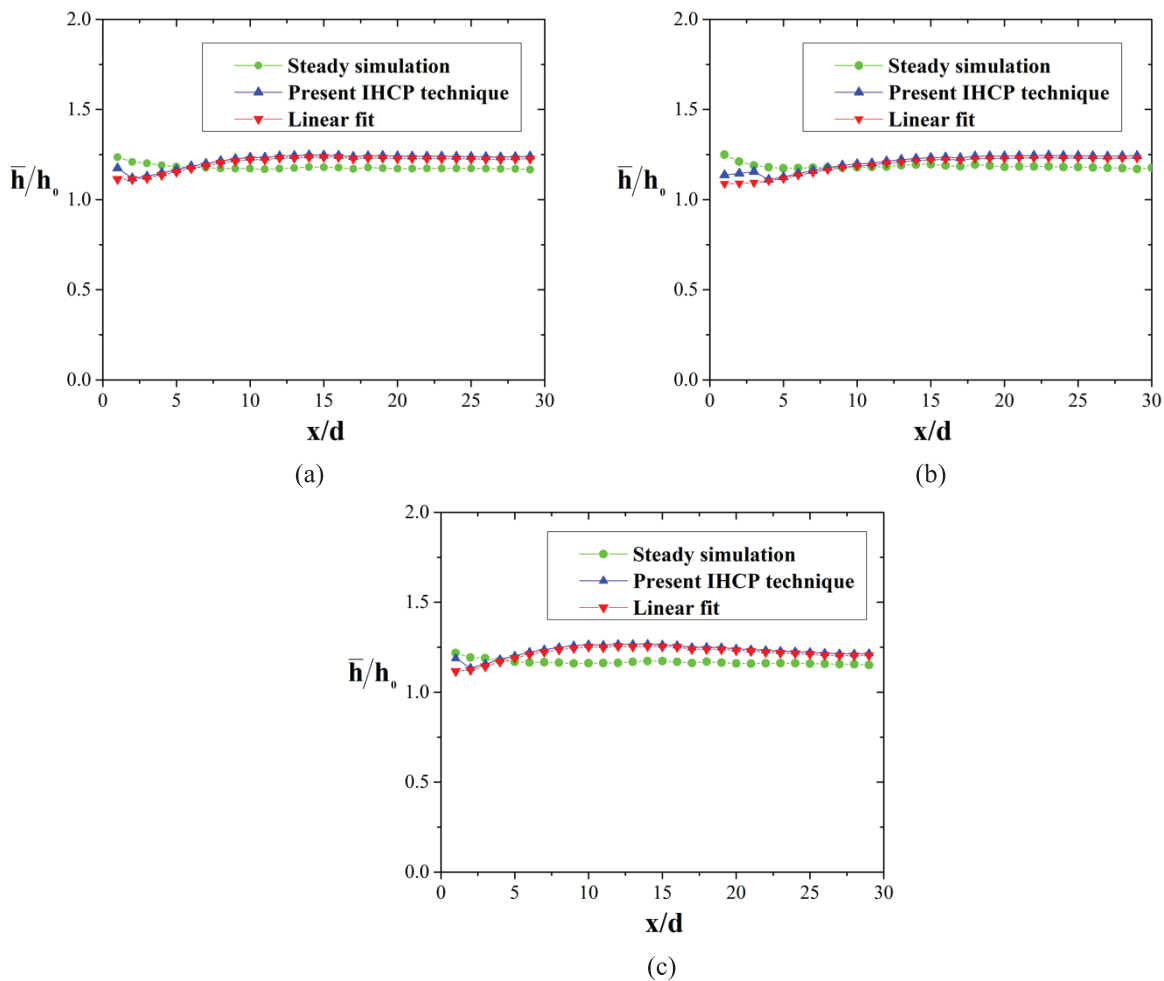


Figure 12. Comparison of normalized laterally averaged heat transfer coefficient obtained using different techniques for (a) $M = 0.5$, (b) $M = 0.8$ and (c) $M = 1.0$.

also used to determine the h_0 . Figure 11 compares the heat transfer coefficient values obtained using the above mentioned methods. The results of the various methodologies demonstrate an excellent agreement with each other, with an average deviation of less than 5%.

Figure 12 shows the normalized laterally averaged heat transfer coefficient values estimated using the present IHCP algorithm for film cooling case for $M = 0.5, 0.8, \text{ and } 1.0$. The figure also includes \bar{h} values obtained from the steady-state simulation and the linear fit method for comparison. A general trend of heat transfer coefficient in film cooling is that it increases with blowing ratio due to higher turbulence generated with an increase in injected coolant mass flux. Also, injection of coolant into the mainstream augments local turbulence levels. Hence, the steady-state simulation exhibits a higher heat transfer rate near the film hole exit and gradually reduces to a more or less constant value along the downstream. The estimated \bar{h} from the IHCP algorithm follows the steady-state simulation results, but it appears to have slightly deviated in the immediate downstream of the jet exit ($x/d < 15$). Further downstream (for $x/d > 15$), the laterally averaged heat transfer coefficient values from all the methods closely agree with each other. The average deviation between the estimated heat transfer coefficient using IHCP and steady-state simulation is observed to be around 4% for all the blowing ratios studied. Results from the linear fit method also followed a similar trend as the IHCP solution with an error of around 3%.

In the region immediately downstream of injection, a maximum deviation of around 9% is observed between the IHCP results and steady-state simulation output. One primary cause of such an anomaly in the current transient approach might be the conjugate heat transfer solution employed in the present simulation. As the coolant passes through the film hole, the plate temperature surrounding the hole might reduce, causing less heat transfer coefficient values near the film hole exit. As a result, it can be concluded that the current method may be more realistic than a steady-state analysis since it includes the effect of heat transfer across the film hole and the plate.

CONCLUSION

The present paper demonstrated a novel approach to simultaneously estimating the thermal boundary parameters of film cooling based on an inverse heat conduction technique. The solution methodology adopted in the present work employs an optimization technique to evaluate film cooling effectiveness and heat transfer coefficient appearing in the analytical solution of the transient one-dimensional semi-infinite model. The transient wall temperature data at the film cooling surface is the only input required for this method and is generated through a three-dimensional numerical simulation for a cylindrical hole film cooling arrangement. The estimated values from the present IHCP method showed good agreement having

a slight deviation of around 7% for the effectiveness and 4% for the heat transfer coefficient. The estimated h values from the present IHCP solution were underpredicted by about 6% for x/d less than 5, where the effect of coolant flow through the film hole prevails. A significant advantage of this technique is that only up to 100 seconds of transient temperature data is sufficient to evaluate both η and h using a single test. One major limitation of the current technique is the accurate calculation of sensitivity coefficients. Also, it can be concluded from the sensitivity analysis that a higher sampling rate while measuring the transient temperature data would reduce the estimation uncertainty. Overall, it can be ascertained from the present work that the IHCP technique can be successfully implemented to simultaneously estimate the effectiveness and heat transfer coefficient for transient film cooling analysis.

NOMENCLATURE

d	Diameter of film cooling hole, mm
h	Heat transfer coefficient, $\text{W}/\text{m}^2\text{K}$
J	Jacobian
k	Thermal conductivity, W/mK
L	Thickness of the plate, mm
M	Blowing ratio
P	Parameter
q''	Heat flux, W/m^2
S	Objective function
T	Temperature, K
t	Time, s
U	Velocity, m/s
x, y, z	Coordinates
Y	Measured data

Greek symbols

α	Thermal diffusivity, m^2/s
η	Effectiveness
λ	Damping parameter

Subscripts

c	Coolant
f	Film cooling
i	Initial
m	Mainstream
ref	Reference temperature
w	Wall

Abbreviations

<i>CRVP</i>	Counter rotating vortex pair
<i>IHCP</i>	Inverse heat conduction problem
<i>LMA</i>	Levenberg-Marquardt algorithm

AUTHORSHIP CONTRIBUTIONS

Authors equally contributed to this work.

DATA AVAILABILITY STATEMENT

The authors confirm that the data that supports the findings of this study are available within the article. Raw data that support the finding of this study are available from the corresponding author, upon reasonable request.

CONFLICT OF INTEREST

The author declared no potential conflicts of interest with respect to the research, authorship, and/or publication of this article.

ETHICS

There are no ethical issues with the publication of this manuscript.

REFERENCES

- [1] Cherrared D. Numerical simulation of film cooling a turbine blade through a row of holes. *J Therm Eng* 2017;3:1110–1120. [\[CrossRef\]](#)
- [2] Akbar M. The effects of coolant pipe geometry and flow conditions on turbine blade film cooling. *J Therm Eng* 2017;3:1196–1210. [\[CrossRef\]](#)
- [3] Han JC, Dutta S, Ekkad S. Gas turbine heat transfer and cooling technology. 2nd ed. Florida: CRC Press; 2012. [\[CrossRef\]](#)
- [4] Goldstein RJ, Eckert ERG, Ramsey JW. Film cooling with injection through holes: adiabatic wall temperatures downstream of a circular hole. *J Eng Power* 1968;90:384–393. [\[CrossRef\]](#)
- [5] Eriksen VL, Goldstein RJ. Heat transfer and film cooling following injection through inclined circular tubes. *J Heat Transf* 1974;96:239–245. [\[CrossRef\]](#)
- [6] Al-Obaidi AR. Investigation of fluid field analysis, characteristics of pressure drop and improvement of heat transfer in three-dimensional circular corrugated pipes. *J Energy Storage* 2019;26:101012. [\[CrossRef\]](#)
- [7] Al-Obaidi AR, Sharif A. Investigation of the three-dimensional structure, pressure drop, and heat transfer characteristics of the thermohydraulic flow in a circular pipe with different twisted-tape geometrical configurations. *J Therm Anal Calorim* 2021;143:3533–3558. [\[CrossRef\]](#)
- [8] Vedula RJ, Metzger DE. A method for the simultaneous determination of local effectiveness and heat transfer distributions in three-temperature convection situations. In: Chulya A, Gyekenyesi JP; Bhatt RT, editors. 36th International Gas Turbine and Aeroengine Congress and Exposition; 1991 June 3-6; Orlando: ASME; 1991.
- [9] Ekkad SV, Zapata D, Han JC. Film effectiveness over a flat surface with air and CO₂ injection through compound angle holes using a transient liquid crystal image method. 1995 International Gas Turbine and Aeroengine Congress and Exposition; 1995 June 5-8; Houston, Texas: ASME; 1995. Article V004T09A011. [\[CrossRef\]](#)
- [10] Ekkad SV, Zapata D, Han JC. Heat transfer coefficient over a flat surface with air and CO₂ injection through compound angle holes using a transient liquid crystal image method. *J Turbomach* 1997;119:580–586. [\[CrossRef\]](#)
- [11] Al-Obaidi AR. Study the influence of concavity shapes on augmentation of heat-transfer performance, pressure field, and fluid pattern in three-dimensional pipe. *Heat Transf* 2021;50:4354–4381. [\[CrossRef\]](#)
- [12] Ekkad SV, Ou S, Rivir RB. A transient infrared thermography method for simultaneous film cooling effectiveness and heat transfer coefficient measurements from a single test. *J Turbomach* 2004;126:597–603. [\[CrossRef\]](#)
- [13] Chen PH, Ding PP, Ai D. An improved data reduction method for transient liquid crystal thermography on film cooling measurements. *Int J Heat Mass Transf* 2001;44:1379–1387. [\[CrossRef\]](#)
- [14] Vogel G, Grat ABA, Von Wolfersdorf J, Weigand B. A novel transient heater-foil technique for liquid crystal experiments on film-cooled surfaces. *J Turbomach* 2003;125:529–537. [\[CrossRef\]](#)
- [15] Xue S, Roy A, Ng WF, Ekkad SV. A novel transient technique to determine recovery temperature, heat transfer coefficient, and film cooling effectiveness simultaneously in a transonic turbine cascade. *J Therm Sci Eng Appl* 2015;7:011016. [\[CrossRef\]](#)
- [16] Ahmed S, Singh P, Ekkad SV. Three-Dimensional transient heat conduction equation solution for accurate determination of heat transfer coefficient. *J Heat Transf* 2020;142:051302. [\[CrossRef\]](#)
- [17] Ekkad SV, Singh P. Liquid crystal thermography in gas turbine heat transfer: A review on measurement techniques and recent investigations. *Crystals* 2021;11:1332. [\[CrossRef\]](#)
- [18] Ozisik MN. Inverse heat transfer: Fundamentals and applications. 1st ed. United Kingdom: Routledge; 2018.
- [19] Beck J V, Blackwell B, Clair Jr CRS. Inverse heat conduction: Ill-posed problems. 1st ed. New York: Wiley; 1985.
- [20] Ozisik MN, Orlande HRB, Kassab AJ. Inverse heat transfer: fundamentals and applications. *Appl Mech Rev* 2002;55:B18–B19. [\[CrossRef\]](#)
- [21] Beck JV, Arnold KJ. Parameter estimation in engineering and science. 1st ed. New York: Wiley; 1977.
- [22] Colaco MJ, Orlande HRB, Dulikravich GS. Inverse and optimization problems in heat transfer. *J Brazilian Soc Mech Sci Eng* 2006;28:1–24. [\[CrossRef\]](#)

- [23] Tahmasbi V, Noori S. Application of Levenberg-Marquardt method for estimation of the thermophysical properties and thermal boundary conditions of decomposing materials. *Heat Transf Eng* 2020;41:449–475. [CrossRef]
- [24] Duda P, Konieczny M. An iterative algorithm for the estimation of thermal boundary conditions varying in both time and space. *Energies* 2022;15:2686. [CrossRef]
- [25] Deveci K, Maral H, Senel CB, Alpman E, Kavurmacioglu L, Camci C. Aerothermal optimization of squealer geometry in axial flow turbines using genetic algorithm. *J Therm Eng* 2018;4:1896–1911. [CrossRef]
- [26] Al-Obaidi AR. Investigation of the flow, pressure drop characteristics, and augmentation of heat performance in a 3D flow pipe based on different inserts of twisted tape configurations. *Heat Transf* 2021;50:5049–5079. [CrossRef]
- [27] Al-Obaidi AR, Chaer I. Study of the flow characteristics, pressure drop and augmentation of heat performance in a horizontal pipe with and without twisted tape inserts. *Case Stud Therm Eng* 2021;25:100964. [CrossRef]
- [28] Al-Obaidi AR. Analysis of the flow field, thermal performance, and heat transfer augmentation in circular tube using different dimple geometrical configurations with internal twisted-tape insert. *Heat Transf* 2020;49:4153–4172. [CrossRef]
- [29] Al-Obaidi AR, Alhamid J, Hamad F. Flow field and heat transfer enhancement investigations by using a combination of corrugated tubes with a twisted tape within 3D circular tube based on different dimple configurations. *Heat Transf* 2021;50:6868–6885. [CrossRef]
- [30] Al-Obaidi AR, Alhamid J. Numerical investigation of fluid flow, characteristics of thermal performance and enhancement of heat transfer of corrugated pipes with various configurations. 2nd International Conference on Trends in Mechanical and Aerospace (TMAE) 2020; 2020 Sept 25–27; Washington: IOP Publishing; 2020. Article 12004.
- [31] Alhamid J, Al-Obaidi RA. Flow pattern investigation and thermohydraulic performance enhancement in three-dimensional circular pipe under varying corrugation configurations. *J Phys Conf Ser* 2021;1845:12061. [CrossRef]
- [32] Al-Obaidi AR. Investigation on effects of varying geometrical configurations on thermal hydraulics flow in a 3D corrugated pipe. *Int J Therm Sci* 2022;171:107237. [CrossRef]
- [33] Al-Obaidi AR, Alhamid J. Investigation of flow pattern, thermohydraulic performance and heat transfer improvement in 3D corrugated circular pipe under varying structure configuration parameters with development different correlations. *Int Commun Heat Mass Transf* 2021;126:105394. [CrossRef]
- [34] Alhamid J, Al-Obaidi AR. Effect of concavity configuration parameters on hydrodynamic and thermal performance in 3D circular pipe using Al₂O₃ nanofluid based on CFD simulation. *J Phys Conf Ser* 2021;1845:12060. [CrossRef]
- [35] Walters DK, Leylek JH. A systematic computational methodology applied to a three-dimensional film-cooling flowfield. *J Turbomach* 1997;119:777–785. [CrossRef]
- [36] Harrison KL, Bogard DG. Comparison of RANS turbulence models for prediction of film cooling performance. ASME Turbo Expo 2008 Power Land, Sea, Air, 2008; 2008 June 9–13; Berlin, Germany: ASME; 2008. pp. 1187–1196.
- [37] Bohn D, Ren J, Kusterer K. Conjugate heat transfer analysis for film cooling configurations with different hole geometries. The 2003 International Joint Power Generation Conference; 2003 June 16–19; Atlanta, Georgia: ASME; 2003. pp. 247–256. [CrossRef]
- [38] Bohn D, Ren J, Kusterer K. Systematic investigation on conjugate heat transfer rates of film cooling configurations. *Int J Rotating Mach* 2005;2005:535907. [CrossRef]
- [39] Humber W, Ni R-H, Johnson J, Clark J, King P. Comparison of conjugate heat transfer analysis of flat plate film cooling arrays against experimental data. ASME Turbo Expo 2015: Turbine Technical Conference and Exposition; 2015 June 15–19; Quebec Canada: ASME; 2015. Article V05AT10A006.
- [40] Hahn DW, Ozisik MN. Heat conduction. 3rd ed. New York: Florida; 2012. [CrossRef]
- [41] Sinha AK, Bogard DG, Crawford ME. Film-cooling effectiveness downstream of a single row of holes with variable density ratio. *J Turbomach* 1991;113:442–449. [CrossRef]
- [42] Azzawi IDJ, Jaworski AJ, Mao X. An overview of synthetic jet under different clamping and amplitude modulation techniques. *J Fluids Eng* 2021;143:031501. [CrossRef]
- [43] Yahya SG, Azzawi IDJ, Abbas MK, Al-Rubaiy AA. Characteristics of acoustic drivers for efficient coupling to thermoacoustic machines. Proceedings of the International MultiConference of Engineers and Computer Scientists 2019; 2019 May 13–15; Hong Kong: Newswood Limited; 2019. pp. 469–474.
- [44] Mahmood OS, Karim AMA, Yahya SG, Azzawi IDJ. Miniaturized traveling-wave thermoacoustic refrigerator driven by loudspeaker: Numerical design. *Int J Air-Conditioning Refrig* 2020;28:2050035. [CrossRef]
- [45] Nellis G, Klein SA. Heat Transfer. Cambridge: Cambridge University Press; 2009. [CrossRef]
- [46] Incropera FP, DeWitt DP, Bergman TL, Adrienne LS. Fundamentals of heat and mass transfer. 6th ed. New York: John Wiley & Sons; 2006.

-
- [47] Kapadia S, Roy S, Heidmann J. Detached eddy simulation of turbine blade cooling. 36th AIAA Thermophysics Conference 2003 June 23-26; Orlando, Florida: ARC; 2003. pp. 1–10. [\[CrossRef\]](#)
- [48] Zhang XZ, Hassan I. Film cooling effectiveness of an advanced-louver cooling scheme for gas turbines. *J Thermophys Heat Transf* 2006;20:754–763. [\[CrossRef\]](#)
- [49] Kadam AR, Hindasageri V, Kumar GN. Inverse estimation of heat transfer coefficient and reference temperature in jet impingement. *J Heat Transf* 2020;142:092302. [\[CrossRef\]](#)